Single-shot non-intercepting profile monitor of plasma-accelerated electron beams with nanometric resolution

A. Curcio, M. Anania, F. Bisesto, E. Chiadroni, A. Cianchi, M. Ferrario, F. Filippi, D. Giulietti, A. Marocchino, F. Mira, M. Petrarca, V. Shpakov, and A. Zigler

---

Articles you may be interested in

Quiver-quenched optical-field-emission from carbon nanotubes
Applied Physics Letters **111**, 133101 (2017); 10.1063/1.5003004

Experimental characterization of the effects induced by passive plasma lens on high brightness electron bunches
Applied Physics Letters **111**, 184101 (2017); 10.1063/1.4999010

Effect of room temperature lattice vibration on the electron transport in graphene nanoribbons
Applied Physics Letters **111**, 133107 (2017); 10.1063/1.4999127

Topology optimized gold nanostrips for enhanced near-infrared photon upconversion
Applied Physics Letters **111**, 133102 (2017); 10.1063/1.4998552

Ion-beam-induced planarization, densification, and exfoliation of low-density nanoporous silica
Applied Physics Letters **111**, 133104 (2017); 10.1063/1.4998193

Clocking plasmon nanofocusing by THz near-field streaking
Applied Physics Letters **111**, 131102 (2017); 10.1063/1.4991860

Single-shot non-intercepting profile monitor of plasma-accelerated electron beams with nanometric resolution

A. Curcio,[1,2,a)] M. Anania,[1] F. Bisesto,[1,2] E. Chiadroni,[1] A. Cianchi,[3] M. Ferrario,[1] F. Filippi,[1,2] D. Giulietti,[4] A. Marocchino,[1] F. Mira,[5] M. Petrarca,[5] V. Shpakov,[1] and A. Zigler[1,6]

[1]*INFN-LNF, via Enrico Fermi 40, 00044 Frascati, Rome*
[2]*Department of Physics, "Sapienza" University of Rome, Piazzale A. Moro 2, I-00185 Rome, Italy*
[3]*INFN and Department of Physics, "Tor Vergata" University, via della ricerca Scientifica 1, 00133 Rome, Italy*
[4]*Physics Department of the University and INFN, Largo Bruno Pontecorvo 3, 56127 Pisa, Italy*
[5]*Department of Basic and Applied Sciences for Engineering (SBAI) and INFN-Roma1, "Sapienza" University of Rome, Via A. Scarpa 14, 00161 Rome, Italy*
[6]*Racah Institute of Physics, Hebrew University, Jerusalem 91904, Israel*

An innovative, single-shot, non-intercepting monitor of the transverse profile of plasma-accelerated electron beams is presented, based on the simultaneous measurement of the electron energy and the betatron radiation spectra. The spatial resolution is shown to be down to few tens of nanometers, important for high-precision applications requiring fine shaping of beams and detailed characterizations of the electron transverse phase space at the exit of plasma accelerating structures. *Published by AIP Publishing.* [http://dx.doi.org/10.1063/1.4998932]

The transverse profile of plasma-accelerated electrons is a primary information in order to qualify the beams and characterize them for different applications. These kinds of beams are accelerated over lengths ranging from millimeters to centimeters where standard intercepting diagnostics, normally exploited in conventional RF accelerators, become non-implementable. Both in the schemes of Laser WakeField (LWFA) and Particle WakeField (PWFA) Acceleration,[1] in the extremely non-linear regime of interaction, the accelerating wakefield assumes the shape of a bubble.[2] Beside the impressively strong longitudinal fields associated with the wake (up to TV/m), the transverse fields in this configuration are much favorable for the acceleration of high-quality beams because of their linear trend, which can preserve efficiently the emittance of the injected electron beams. Furthermore, these transverse focusing fields are responsible for intra-envelope betatron oscillations of electrons,[3] whence the so-called betatron radiation is produced.[4] Because of relativistic effects, the betatron radiation spectrum normally extends over the X-ray region of the electromagnetic spectrum.[5,6] The use of betatron radiation as transverse diagnostics for electron beams accelerated in plasmas is to date largely diffused and demonstrated.[7–11] The main advantages associated with this diagnostics are two: it is not destructive/intercepting and it can work for single-shot experiments due to its high flux. Since there is no general reason for the beam envelope to be unaffected by the passage from the plasma into vacuum, the use of intercepting diagnostics in vacuum, just after the plasma, is not generally reliable if the goal is that to infer information about the beam while it was accelerating. Intercepting diagnostics implemented outside the plasma like scintillator screens, or even non-intercepting techniques like, for example, those based on diffraction radiation,[12] cannot be considered of practical utilization whenever the electron beam profile is modified at the exit of the plasma in virtue of a smooth (on the scale of a betatron wavelength) plasma-vacuum interface or because of possible space-charge effects. Concerning the determination of the rms beam size inside the plasma, different works have been performed in the recent past, based on Fresnel X-ray diffraction by sharp metallic edges and by X-ray spectroscopy of betatron radiation,[7–11] with an uncertainty very close to 1 μm or, at the best, slightly below. Nevertheless for high-precision applications requiring fine transverse shaping and controlling of electron beams, the complete spatial distribution of the charge is needed more than just the beam's rms size. A high-resolution determination of the beam profile is necessary also for a detailed characterization of the electron transverse phase space at the exit of plasma, whenever the beam has to be exploited for interactions with matter (inverse Compton scattering, irradiation, generation of coherent secondary radiation, etc.) or it has to be matched to and transported through dedicated optics.[13] The only way to directly determine the beam transverse distribution starting from the betatron radiation would be the X-ray imaging of the whole spectrum emitted by the accelerated electrons. On the other hand, being the betatron radiation extremely broadband, it would be not trivial not to lose information and signal when using standard X-ray optics such as Kirckpatrick-Baez mirrors, Bragg crystals, pin-hole cameras, Fresnel lenses, or polycapillary lenses, due to structural limits related to frequency-selection, absorption, aberrations, etc., appropriate of all the above-mentioned devices. Therefore, we propose an innovative technology based on the single-shot spectral detection of both the betatron radiation and the electron beam energy.

The experiment has been performed at the SPARC_LAB test facility via the interaction of the ultra-short ultraintense Ti:Sa laser FLAME with a He gas-jet target, in the bubble regime of the LWFA. It has been shown in Ref. 14 that the

a)alessandro.curcio@lnf.infn.it

laser-plasma system in the bubble regime is associated with an unique matrix $S(I_0, \lambda_0, n_0, \Gamma(\gamma)) \equiv S_{ij}$, depending only on the laser intensity and wavelength, I_0 and λ_0, respectively, on the background electron plasma density n_0, and being a functional of the spectrum $\Gamma(\gamma)$ of the accelerated electrons, with γ the electron Lorentz factor. For a detailed definition of the S-matrix, we refer to Ref. 14, focusing from now on only on the description of our methods and results. The S-matrix can be related to the measured betatron spectrum Σ via the equation

$$D_j \equiv r^i P^i S_{ij} - \Sigma(E_j) = 0, \qquad (1)$$

which is nothing but the statement that the theoretical spectrum must be equal to the detected one. In Eq. (1), the Einstein summation convention has been used, where r_i is the ith betatron oscillation amplitude chosen in some reasonable range of values $[0, r_{max}]$ and P_i is the vector representing the beam's radial profile. The first addendum of Eq. (1), i.e., $r^i P^i S_{ij}$, represents the theoretical betatron radiation spectrum calculated by summing up all the contributions coming from electrons belonging to a beam with a charge spatial distribution P^i. The presence of r^i in the sum comes from the Jacobian determinant for cylindrical coordinates.[4] The detected spectrum is a vector $\Sigma(E_j)$, where the j-index runs over the values of the detected photon energies E_j, being the step $E_{j+1} - E_j = dE$ equal to the resolution of the X-ray detector. The flowchart of our methodology is shown in Fig. 1. Once the laser parameters, the electron plasma density, and the spectrum of the accelerated electrons are experimentally known, the S-matrix can be numerically built.[14] The measured electron and betatron spectra are given as input to the algorithm, which combines the betatron spectrum $\Sigma(E_j)$ with the S-matrix through Eq. (1), yielding the electron beam profile as output. The algorithm is a least-square algorithm which looks for the vector P_i minimizing the norm of the difference vector D_j, defined by Eq. (1).

For sake of clarity, the first approach given in this letter is one-dimensional, and by consequence, we have selected a special case where the laser and the plasma were matched together in such a way to produce an electron beam with cylindrical symmetry, suitable for our 1D approximation. This was accomplished by having control of the geometrical aberrations in the laser focus and also matching the length of the laser pulse to the electron plasma density for avoiding the regime of Direct Laser Acceleration (DLA).[15] For a laser pulse length shorter than the bubble radius, the electrons can be accelerated up to the dephasing point without significantly interacting with the tail of a linearly polarized laser, so without generating an asymmetry both in the electron beam and in the betatron radiation beam. The symmetry of the beams was checked by detecting the spatial distribution of the betatron radiation. In fact, the angular distribution of the betatron radiation is known to be related to the electron trajectories inside the plasma bubble, therefore also to the geometry of the beam while it is evolving during the acceleration. A circular spot of betatron radiation indicates a radially symmetric electron beam. The error on the final electron profile we were able to reconstruct was estimated by taking into account of the errors associated with the betatron spectrum,

FIG. 1. Flowchart of the method for the electron beam profile monitor: once the laser and plasma parameters are experimentally known, the S-matrix of the system can be determined. The measured electron energy and betatron radiation spectra are given as input to the algorithm, yielding the electron beam profile as output.

the electron spectrum, the laser intensity and bandwidth, the electron plasma density, and to the algorithm itself. In particular, the electron energy spectrum, as well as the betatron radiation spectrum, was affected by errors due to finite resolution of the detectors and to the amplitude of the noise fluctuations. The algorithm was affected by an error fixed by an arbitrary threshold for the minimization process and also related to the role of the parameter r_{max} in the convergence of the result. Concerning the resolution of our detector, it was as small as tens of nanometers, as it is shown in the following. The setup of the experiment is reported in Fig. 2. The main laser pulse characteristics during the experiment were $\sim$1 J energy, delivered in 30 fs (FWHM) over a 5 μm rms focus. The laser was focused on a He gas-jet target. The electron density of the generated plasma was measured through a Mach-Zender interferometer to be $n_0 = (2 \pm 0.2) \times 10^{19}$ cm^{-3} (see the up-right inset of Fig. 2). The energy spectrum of the electrons was measured by using a magnetic dipole coupled to a scintillator screen. The betatron radiation emitted by the accelerated electrons during the interaction of the high-intensity laser with the He plasma was detected simultaneously both by a X-ray scintillator and a CCD-X camera, positioned at 0.7 m from the interaction point, cooled down to $-30\,^\circ$C, and shielded by a lead cage from broad-divergence bremsstrahlung. The goal was to measure simultaneously the spatial distribution of the radiation with the X-ray scintillator and the spectrum with the CCD-X camera working in single photon counting mode. The X-ray scintillator was positioned in front of the CCD-X at 0.5 m from the interaction point. The betatron X-ray flux had to cross an overall absorbing thickness constituted by a 280 μm kapton window, a 200 μm X-ray scintillator screen, and 1 μm Al filter to screen the residual infrared light on the camera. The spectra of the betatron radiation (already deconvolved with the transmission function of the filters) and of the electron energies are reported in the up-left and the bottom insets, respectively, of Fig. 2. We used these spectra as input for our algorithm, finally getting the result reported in Fig. 3. The 1D radially symmetric profile is relative to a beam of sub-μm size, rms 250 nm.

When referring to Eq. (1), for a square matrix S_{ij}, the number of components of the solution vector P_i in the range $[0, r_{max}]$ is as much as the components of the vector Σ_j, which represents the detected spectrum. The number of components of the vector Σ_j is determined by the dynamic range and the resolution of the X-ray spectrometer. For the laser and plasma parameters of our experiments, we expected a r_{max} parameter of about $\sim$1 μm, since the scaling laws for betatron radiation[16] gave hint for a submicrometric beam's rms
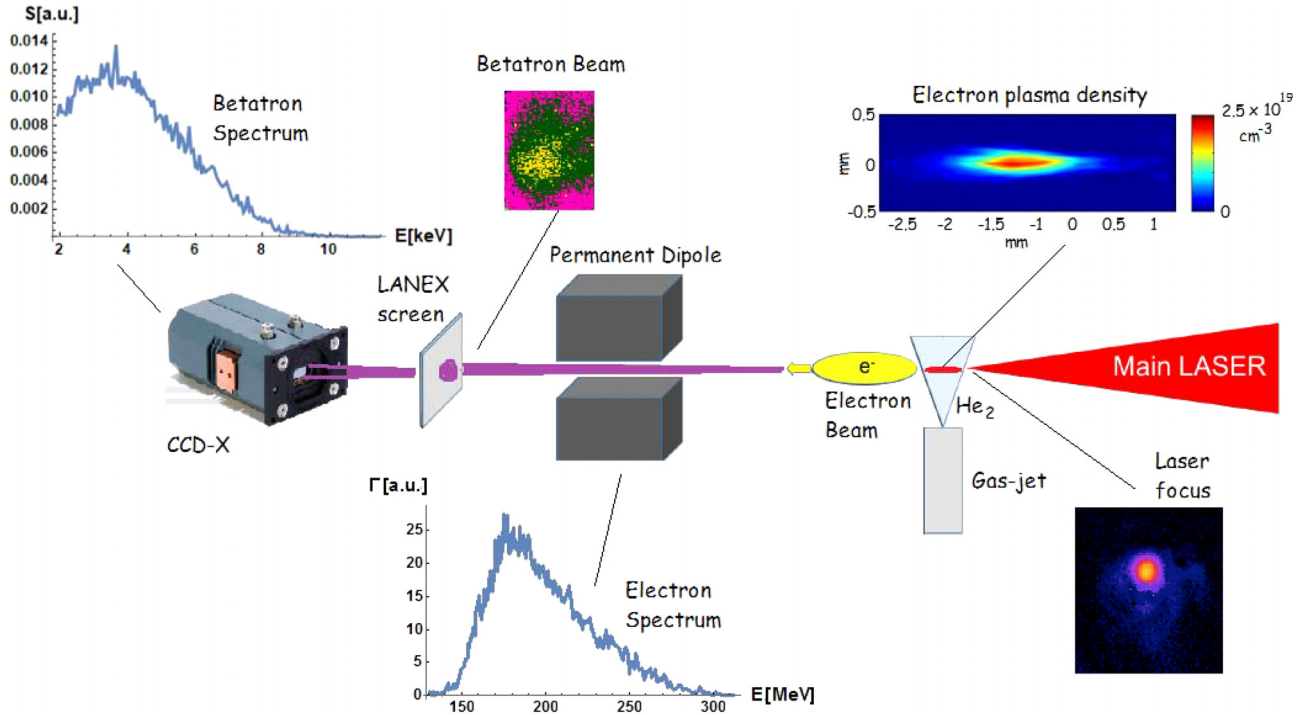
FIG. 2. The laser beam is focused on the He gas-jet. Electrons are accelerated in the bubble regime over a distance $\gtrsim 1$ mm. The permanent dipole ($\lesssim 1$ T) coupled with a scintillator screen allows the measurement of the electron energy spectrum. The X-ray betatron radiation, directed in the same direction of the impinging laser, crosses an X-ray scintillator and then it gets the X-ray spectrometer. A probe beam is coupled to a Mach-Zender interferometer in order to retrieve the electron plasma density of the laser-produced plasma.

size. The number of components of Σ_j in our particular case was 140. The best resolution achievable by reasoning in these terms was therefore $1\mu m/140 \sim 7$ nm. This resolution would be very high, and, in principle, our method would be able to provide it. Nevertheless the relative error affecting the coefficients of the S-matrix was >10%, falling from the experimental determination of the electron plasma density, the laser intensity, and the electron energy spectrum. Considering that the rms size of the retrieved beam was 250 nm, a 7 nm resolution would set a relative error of about 3%, less than the error related to the S-matrix. For this reason, the 7 nm resolution had no empirical significance and a more reasonable estimation of the resolution should be done. Once ensured that the code was stable with respect to small variations of the r_{max} parameter, we gradually reduced the number of components of the vector Σ_j with a decimation procedure, until the reconstructed electron profile (the output of our analysis code) started to show modifications, in particular, in the rms size. This threshold number of points was used to define a more realistic resolution for the profile monitor. The resolution found in this case sets a relative error of about 16%. A lower resolution (>40 nm) could bring to an erroneous result, not consistent with the scaling laws of betatron radiation and numerically unstable (i.e., unreliable). Therefore, we finally concluded that the resolution of our monitor was 40 nm. The fact that the result of our measurement was quite smooth (by the way not perfectly Gaussian if carefully looking) was due at least to two main reasons. The first one is that the geometry and symmetry of interaction was highly cylindrical with no particular inhomogeneity/anisotropy in the laser focus and in the plasma profile; thus, no microstructures and asymmetries had to be expected in

the profile of the accelerated electrons. The second reason was that during our measurement, we adopted the 1D version of the method, which naturally averaged out asymmetries or microstructures, even if any. Actually, there was a further smoothing factor, not so easy to argue at first sight: our monitor is time-integrated on the acceleration time (this is automatically taken into account through the choice of the betatron trajectories for the determination of the matrix S_{ij}, see Ref. 14); therefore, any transient beam microstructure was necessarily averaged out. Despite the monitor was time-integrated over the duration of the electron acceleration inside the bubble, since the emitted power of betatron radiation scales as $\gamma^{3/2}$,[16] it was possible to be confident that the profile of Fig. 3 referred more to the last phase of acceleration (basically around the exit of the plasma accelerating
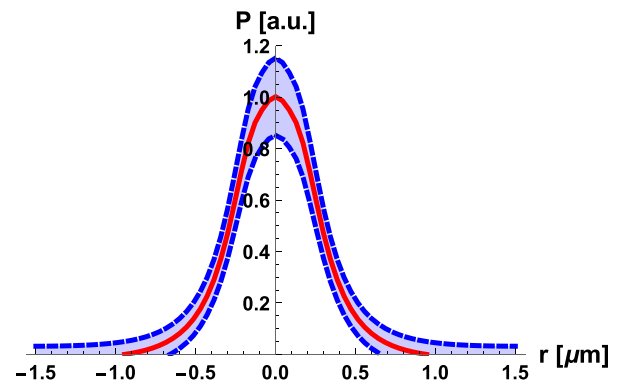

FIG. 3. Beam profile detection in the radial approximation (red curve). The blue curves delimit the error range. The beam's rms size $\sigma_r = 0.25 \pm 0.04 \mu$m. The monitor resolution is 40 nm.
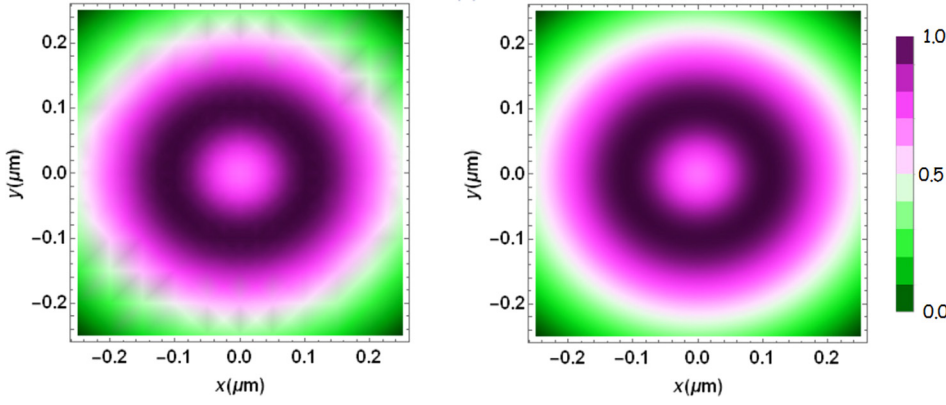
FIG. 4. Retrieved electron profile (left) and ideal elliptic-hollow electron beam profile (right). Monitor resolution: 50 nm (pixel size: $50 \times 50 \, nm^2$).

structure, where the energy gain was supposed to be maximum) then to the precedent ones.

The idea to overcome the 1D approximation and to design a 2D beam profile detector is related to another algebraic problem, very similar to the problem of Eq. (1), which involves now the use of a fourth rank tensor. The S-matrix can be extended to a 4th rank tensor when considering that the electron independent coordinates in the transverse plane are in general two (r, ϕ) with ϕ the azimuth angle, and also the spectrum of radiation depends on two variables that are the photon energy and the solid angle Ω, as expressed in following equation:

$$D_{kl} \equiv r^i P^{ij} S_{ijkl} - \Sigma(E_k, \Omega_l) = 0. \qquad (2)$$

Now the matrix P_{ij} represents the 2D beam profile matrix with i representing the radial coordinate and j the azimuth. The index k runs over the detected photon energies and l over the solid angle within which the radiation spectrum is collected. A 2D beam profile monitor based on Eq. (2) could be therefore possible only when the correlated angular-spectral distribution of the betatron radiation is detected. This last task is not trivial to accomplish because it requires the detection of the X-ray spectrum in different regions of the X-ray beam spot. Some work has already been done in this sense by exploiting stacks of imaging plates to characterize the angular dependence of the critical energy of the synchrotron-like betatron spectrum.[17] In our experiment, with our diagnostics, we were not able to perform the same measurements as in Ref. 17. Nevertheless we aim to demonstrate in the following the feasibility of our 2D beam monitor through a numerical simulation. In order to shed more light on the resolution capability of our monitor, a numerical example was prepared. It was decided to retrieve the profile of an elliptic-hollow electron beam, whose internal diameter was below 100 nm in both planes. The ellipticity was meant to demonstrate the 2D operation of the retrievement procedure, while the hole in the beam was thought to be useful to show the resolution performances of the monitor. The spectral-angular distribution of betatron radiation $\Sigma(E_k, \Omega_l)$ was determined through formulas reported in Ref. 4 for a fictitious electron beam having the same energy-spectrum shown in Fig. 2, and for the same laser and plasma parameters used earlier. A reasonable number of points (ten) was chosen in the range $[0, \Omega_{max}]$ for the solid angle, simulating a realistic measurement in which for logistic/technological issues it

would be not possible to detect the betatron spectrum in correspondence of an arbitrary number of solid angles. The linear size of the pixel, i.e., the monitor resolution, of our detector was $2 \times x_{max}/10 = 2 \times y_{max}/10 = 500 \, nm/10 = 50 \, nm$, where x_{max} and y_{max} are the parameters defining half of the x and y position ranges, respectively. In Fig. 4, the result of our simulation is shown. The ellipticity and the hole at the center of the beam were resolved with an accuracy of tens of nanometers. In the case of a real experiment, the increase of angular resolution of the betatron radiation detection apparatus could bring to even finer resolution performances of the monitor, nevertheless provided that the relative error (given by the ratio between the resolution and the rms sizes) has empirical significance. This has been properly pointed out earlier when discussing our measurements and it consists in the real limit of the diagnostics, which in principle could provide any desired resolution just by refining the angular sampling of the betatron radiation distribution.

The 2D beam profile monitor as conceived in this letter is naturally a beam position monitor as well. In fact, following the X-ray beam position on the X-ray scintillator gives indications on the relative position shot-to-shot of the electron beam, due to the collimation properties of the betatron radiation. In conclusion, we reported on an innovative technological conception for a beam profile/position monitor based on betatron radiation, suitable for electron beams accelerated in the bubble regime of plasma acceleration. Our fundamental achievement was to demonstrate a high-resolution down to few tens of nanometers, for a monitor which is non-intercepting, non-destructing, and revealing good performances in single-shot experiments. Our result is a large improvement with respect to other beam diagnostics based on betatron radiation to date, paving the way to fine transverse shaping (down to nanometric scale) of beams and detailed characterizations of the transverse phase space of plasma-accelerated electrons.

[1]E. Esarey, C. B. Schroeder, and W. P. Leemans, "Physics of laser-driven plasma-based electron accelerators," Rev. Mod. Phys. **81**, 1229 (2009).

[2]A. Pukhov, S. Gordienko, S. Kiselev, and I. Kostyukov, "The bubble regime of laser–plasma acceleration: Monoenergetic electrons and the scalability," Plasma Phys. Controlled Fusion **46**, B179 (2004).

[3]S. Corde, K. Ta Phuoc, G. Lambert, R. Fitour, V. Malka, A. Rousse, A. Beck, and E. Lefebvre, "Femtosecond x rays from laser-plasma accelerators," Rev. Mod. Phys. **85**(1), 1 (2013).

[4]E. Esarey, B. A. Shadwick, P. Catravas, and W. P. Leemans, "Synchrotron radiation from electron beams in plasma-focusing channels," Phys. Rev. E **65**, 056505 (2002).

[5]A. Rousse, K. Ta Phuoc, R. Shah, A. Pukhov, E. Lefebvre, V. Malka, S. Kiselev, F. Burgy, J. Rousseau, D. Umstadter, and D. Hulin, "Production of a keV X-ray beam from synchrotron radiation in relativistic laser-plasma interaction," Phys. Rev. Lett. **93**(13), 135005 (2004).

[6]S. Wang, C. E. Clayton, B. E. Blue, E. S. Dodd, K. A. Marsh, W. B. Mori, C. Joshi, S. Lee, P. Muggli, T. Katsouleas, F. J. Decker, M. J. Hogan, R. H. Iverson, P. Raimondi, D. Walz, R. Siemann, and R. Assmann, "X-ray emission from betatron motion in a plasma wiggler," Phys. Rev. Lett. **88**(13), 135004 (2002).

[7]S. Kneip, C. McGuffey, J. L. Martins, M. S. Bloom, V. Chvykov, F. Dollar, R. Fonseca, S. Jolly, G. Kalintchenko, K. Krushelnick, A. Maksimchuk, S. P. D. Mangles, Z. Najmudin, C. A. J. Palmer, K. Ta Phuoc, W. Schumaker, L. O. Silva, J. Vieira, V. Yanovsky, and A. G. R. Thomas, "Characterization of transverse beam emittance of electrons from a laser-plasma wakefield accelerator in the bubble regime using betatron x-ray radiation," Phys. Rev. Spec. Top.–Accel. Beams **15**(2), 021302 (2012).

[8]G. R. Plateau, C. G. R. Geddes, D. B. Thorn, M. Chen, C. Benedetti, E. Esarey, A. J. Gonsalves, N. H. Matlis, K. Nakamura, C. B. Schroeder, S. Shiraishi, T. Sokollik, J. van Tilborg, C. Toth, S. Trotsenko, T. S. Kim, M. Battaglia, T. Stohlker, and W. P. Leemans, "Low-emittance electron bunches from a laser-plasma accelerator measured using single-shot x-ray spectroscopy," Phys. Rev. Lett. **109**(6), 064802 (2012).

[9]M. Schnell, A. Savert, B. Landgraf, M. Reuter, M. Nicolai, O. Jackel, C. Peth, T. Thiele, O. Jansen, A. Pukhov, O. Willi, M. C. Kaluza, and C. Spielmann, "Deducing the electron-beam diameter in a laser-plasma accelerator using X-ray betatron radiation," Phys. Rev. Lett. **108**(7), 075001 (2012).

[10]F. Albert, R. Shah, K. Ta Phuoc, R. Fitour, F. Burgy, J. Rousseau, A. Tafzi, D. Douillet, T. Lefrou, and A. Rousse, "Betatron oscillations of electrons accelerated in laser wakefields characterized by spectral x-ray analysis," Phys. Rev. E **77**(5), 056402 (2008).

[11]D. B. Thorn, C. G. R. Geddes, N. H. Matlis, G. R. Plateau, E. H. Esarey, M. Battaglia, C. B. Schroeder, S. Shiraishi, T. Stohlker, C. Tóth, and W. P. Leemans, "Spectroscopy of betatron radiation emitted from laser-produced wakefield accelerated electrons," Rev. Sci. Instrum. **81**(10), 10E325 (2010).

[12]A. Cianchi, M. Castellano, L. Catani, E. Chiadroni, K. Honkavaara, and G. Kube, "Nonintercepting electron beam size monitor using optical diffraction radiation interference," Phys. Rev. Spec. Top.–Accel. Beams **14**(10), 102803 (2011).

[13]J. van Tilborg, S. Steinke, C. G. R. Geddes, N. H. Matlis, B. H. Shaw, A. J. Gonsalves, J. V. Huijts, K. Nakamura, J. Daniels, C. B. Schroeder, C. Benedetti, E. Esarey, S. S. Bulanov, N. A. Bobrova, P. V. Sasorov, and W. P. Leemans, "Active plasma lensing for relativistic laser-plasma-accelerated electron beams," Phys. Rev. Lett. **115**(18), 184802 (2015).

[14]A. Curcio, M. Anania, F. Bisesto, E. Chiadroni, A. Cianchi, M. Ferrario, F. Filippi, D. Giulietti, A. Marocchino, M. Petrarca, V. Shpakov, and A. Zigler, "Trace-space reconstruction of low-emittance electron beams through betatron radiation in laser-plasma accelerators," Phys. Rev. Accel. Beams **20**(1), 012801 (2017).

[15]A. Pukhov and J. Meyer-ter-Vehn, "Laser wake field acceleration: The highly non-linear broken-wave regime," Appl. Phys. B **74**(4–5), 355–361 (2002).

[16]A. G. R. Thomas, "Scalings for radiation from plasma bubbles," Phys. Plasmas **17**(5), 056708 (2010).

[17]F. Albert, B. B. Pollock, J. L. Shaw, K. A. Marsh, J. E. Ralph, Y.-H. Chen, D. Alessi, A. Pak, C. E. Clayton, S. H. Glenzer, and C. Joshi, "Angular dependence of betatron x-ray spectra from a laser-wakefield accelerator," Phys. Rev. Lett. **111**(23), 235004 (2013).